*Graphical Abstract

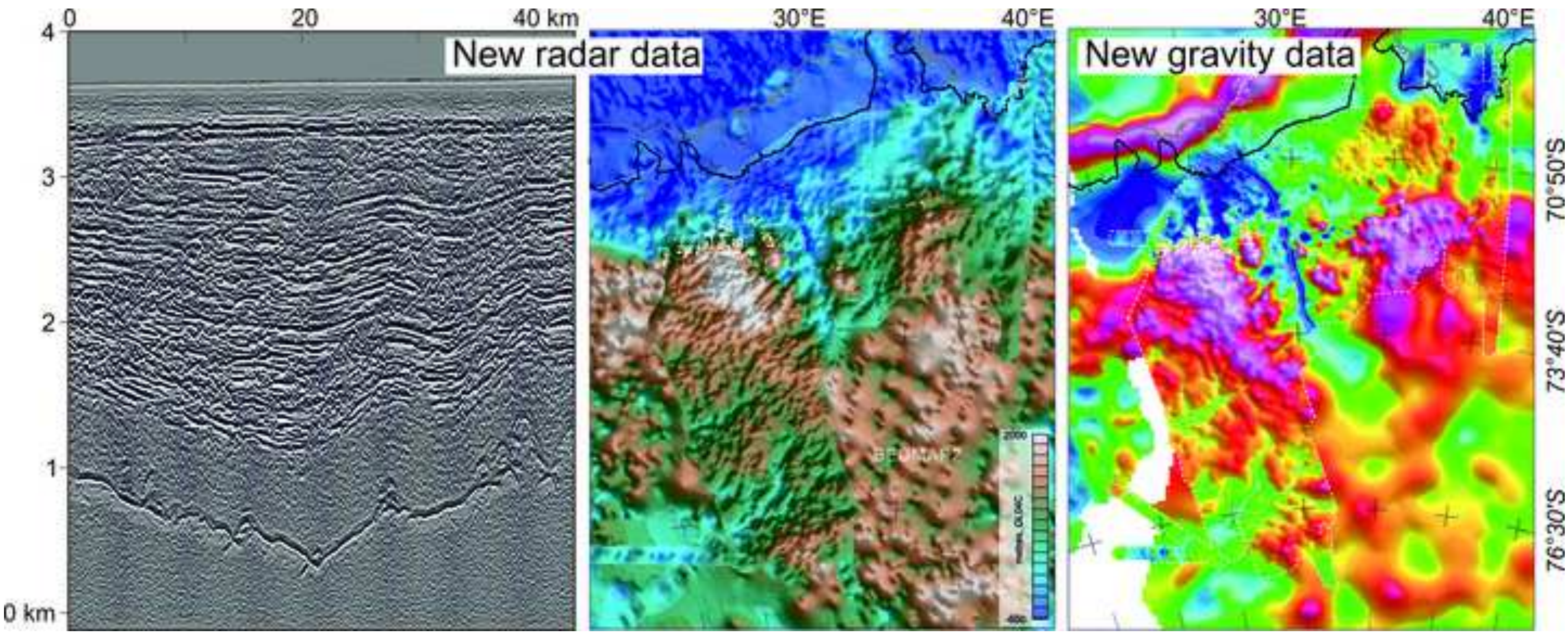

Highlights:

Nearly 40000 km of new gravity and radar data in eastern Dronning Maud Land

Paleo-fluvial drainage system behind great escarpment experienced short-lived phase of alpine glaciation preceding present cold-based era

Offshore sediments derived from erosion of material by balanced backwearing and downwearing seawards of a breakup-aged or older (i.e. Jurassic) inland drainage divide

Paleo-fluvial drainage system may therefore be very ancient

Longer-distance sediment transport in Jurassic river system further east via a valley now glacially deepened to form a Grand Canyon-sized subglacial trough

Erosion at extended continental margins: insights from new aerogeophysical data in eastern Dronning Maud Land

Graeme Eagles[1*], Nanna B. Karlsson[1#], Antonia Ruppel[2], Daniel Steinhage[1], Wilfried Jokat[1,3] and Andreas Läufer[2]

[1]Alfred Wegener Institut, Helmholtz Zentrum für Polar and Meeresforschung
Am Alten Hafen 26
27568 Bremerhaven
Germany

[2]Federal Institute for Geosciences and Natural Resources
Geozentrum Hannover
Stilleweg 2
D-30655 Hannover
Germany

[3]Department of Geosciences
Klagenfurter Str. 4
University of Bremen
Bremen
D-28359 Bremen
Germany

[*]Corresponding author email: graeme.eagles@awi.de
[#]Now at: Geological Survey of Denmark and Greenland, Øster Voldgade 10, 1350 Copenhagen, Denmark

ABSTRACT

Modelling-, rock cooling-, sedimentation- and exposure-based interpretations of the mechanisms by which topography evolves at extended continental margins vary widely. Observations from the margin of Dronning Maud Land, Antarctica, have until now not strongly contributed to these interpretations. Here, we present new airborne gravity and radar data describing the eastern part of this margin. Inland of a tall (2.5 km) great escarpment, a plateau topped by a branching network of valleys suggests preservation of a fluvial landscape with SW-directed drainage beneath a cold-based ice sheet. The valley floor slopes show that this landscape was modified during a period of alpine-style glaciation prior to the onset of the current cold-based phase around 34 Ma. The volume of sediments in basins offshore in the Riiser-Larsen Sea balances with the volume of rock estimated to have been eroded and transported by north-directed drainage from between the escarpment and the continental shelf break. The stratigraphy of these basins shows that most of the erosion occurred during the ~40 Myr following late Jurassic continental breakup. This erosion is unlikely to have been dominated by backwearing because the required rate of escarpment retreat to its present location is faster than numerical models of landscape evolution suggest to be possible. We suggest an additional component of erosion by downwearing seawards of a pre-existing inland drainage divide. The eastern termination of the great escarpment and inland plateau is at the West Ragnhild trough, a 300 km long, 15-20 km wide and up to 1.6 km deep subglacial valley hosting the West Ragnhild glacier. Numerous overdeepened (by >300 m) segments of the valley floor testify to its experience of significant glacial erosion. Thick late Jurassic and early Cretaceous sediments fanning out from the trough's mouth into the eastern Riiser-Larsen Sea betray an earlier history as a river valley. The lack of late Jurassic relief-forming processes in this river's catchment in the interior of East Antarctica suggests this erosion was related to regional climatic change.

Keywords:

airborne gravimetry; airborne radar; great escarpment; extended continental margin; subglacial topography

1. INTRODUCTION

1.1 Background and rationale

Facing the oceans, and several hundred metres to three kilometres in height, so-called great escarpments are known from numerous extended continental margins worldwide (e.g. southern Africa, Brazil, eastern Australia, the Red Sea, and western India). Their presence or absence appears not to correlate with margin age, attesting to their longevity (Gilchrist and Summerfield, 1990). This in turn is linked to the escarpments' roles as drainage divides, by which they sustain feedbacks between climate, erosion, tectonics and isostasy (e.g. Matmon et al., 2002; Sacek et al., 2012). Ideas about the evolution of great escarpment relief vary based on modelling and observation but, as a starting condition, all require the presence or generation of high topography (Braun, 2018). The majority of studies, acknowledging the extended continental margin setting, relate this topography to tectonic processes. Some emphasise the role of normal faulting (e.g. King, 1953; Beaumont et al., 2000). Others focus on flexural-isostatic responses to rifting-related loading of the lithosphere (e.g. Ollier, 1984; Cockburn et al, 2000; Fleming et al, 1999; Gilchrist and Summerfield, 1994; Sacek et al., 2012).

Long-term erosion rates increase strongly following the creation of relief and in response to changes in weathering regimes (e.g. Koppes and Montgomery, 2009). These factors may develop in feedback with one another, but weathering regimes can also alter independently as a consequence of regional or global climatic or tectonic changes. Consistent with the former, the fills of sedimentary basins offshore of the Gondwanan escarpments all seem to have experienced rapid sediment accumulation early on in their histories following the creation of relief by extensional tectonics (Rust & Summerfield, 1990; Gunnell and Fleitout, 1998; Campanile et al., 2008; Rouby et al., 2009; Guillocheau et al., 2011). In these studies, detailed interpretation of the processes by which extended continental margins are shaped by erosion is hampered by the recognition of later accumulation pulses, which can be related to drainage capture events and the evolution of dynamic topography in escarpment hinterlands.

Utilizing onshore evidence instead, geomorphological studies have long concluded that so-called backwearing dominates erosion at extended continental margins. Backwearing involves erosion to base level by intensive gorge incision into escarpments; the escarpments retreat without changing their slope. The observation of multiple regional escarpments and terraces at some margins has led to interpretations of backwearing occurring in cycles modulated by tectonic and climatic changes on geological timescales (e.g. Partridge and Maud, 1987). The idea of cyclicity is consistent with the variable escarpment retreat rates interpreted worldwide from low temperature geochronology and rock exposure dating, which in many instances are an order of magnitude slower than might be required to attain present-day escarpment—shelf distances by constant rates of post breakup retreat (e.g. Brown et al., 1990; Cockburn et al., 2000; Heimsath et al., 2006; Kounov et al., 2007; Mandal et al., 2015; Wildman et al., 2016). Despite this, the spatial and depth resolutions of many low temperature geochronology data sets cannot unequivocally depict rapid escarpment retreat, and alternative scenarios have been preferred where sufficient resolution does exist (Braun and van der Beek, 2004). In addition, numerical landscape evolution models have failed to produce very fast (>1 km/Myr) retreat rates or large sustained changes in retreat rate as a response to any physical process (e.g. Braun, 2018).

Most of the types of studies described above remain to be applied for the continental margin of Dronning Maud Land, Antarctica. Low temperature geochronology data from both ends of the escarpment reveal periods of cooling that can be related to denudation shortly after continental breakup (Jacobs et al. 1992; 1995; Näslund, 2001; Krohne, 2017). As elsewhere in the world, however, the spatial and depth resolutions of these data are not sufficient to unequivocally support the idea of escarpment retreat by erosional backwearing. Using new aerogeophysical data sets, we describe the eastern end of the great escarpment and its surroundings at much higher resolution than possible with previous data sets. Based on our findings, we investigate independently the setting and pattern of erosion and sedimentation each side of the continental margin. We first present a volume-balancing test of the first-order idea that rocks were eroded from the eastern part of the great escarpment and transported as sediments over the shelf and into the deep Riiser-Larsen Sea (Fig. 1). To this end, we combine our aerogeophysical observations with estimates of the volume of clastic material in sediments sampled by marine seismic data. Using the same offshore data set, we interpret the history of sediment accumulation in terms of the pattern and timing of erosion that would have been necessary onshore to produce it.

1.2 Geological history of Dronning Maud Land and the Riiser-Larsen Sea

Mountains of the Sør Rondane region provide the few rocks from which the geological history of eastern Dronning Maud Land has been interpreted (Fig. 1). This history starts in the

1.0-0.5 Ga period with the accretion of multiple juvenile arc terranes between cratonic parts of Africa and East Antarctica (Jacobs et al., 2015; Ruppel et al., 2018). Accretion culminated in the amalgamation of Gondwana. The next major event was the supercontinent's breakup in Jurassic times. This is interpreted from magnetic, gravity and seismic evidence for igneous and volcanic rocks at the region's extended continental margin and in the deep ocean basins of the Lazarev and Riiser-Larsen seas (Riedel et al., 2013; Eagles and König, 2008; Leinweber and Jokat, 2012). These rocks have not been dated directly, but magnetic anomaly isochrons offshore show that seafloor spreading was underway by 160 Ma at the latest, and conceivably earlier (Leinweber and Jokat, 2012). Following this, the only rock-based record of the region's geological history until the development of the East Antarctic ice sheet comes from the low temperature geochronology work of Krohne (2017). Paleotopographic modelling (Wilson et al., 2012) depicts high elevations in Dronning Maud Land around the Eocene-Oligocene transition at 34 Ma, so that it acted as a nucleation zone for the East Antarctic ice sheet as global climate cooled (DeConto & Pollard, 2003). In mid-Miocene times, further cooling led to an increase in ice thickness that has been maintained ever since (Shevenell et al., 2004; Holbourn et al, 2005).

Ice streams flow over short distances towards the present-day continental shelf from the area north of Sør Rondane. Further east, longer-distance ice transport occurs via the West Ragnhild glacier, which originates inland of a gap between Sør Rondane and the Belgica Mountains (Figs. 1,2) to drain a rectangular catchment of ~140000 km^2 (Rignot et al, 2011; Callens et al., 2015). Based on sparse existing radar observations (Siegert, 2005) and thermomechanical ice-sheet models (Pattyn, 2010), the base of this part of the East Antarctic ice sheet is thought not to experience widespread pressure melting. The ice sheet south of Sør Rondane thus remains frozen to its bed, limiting its capacity to erode, and leaving open the possibility for landscape preservation. The subglacial topography and geology, however, are only incompletely known from Soviet aerogeophysical data collected along widely spaced (25—50 km) flight lines flown without continuous satellite navigation. These data are widely known via their contributions to Antarctic radio echo sounding (BEDMAP2), gravity (AntGG) and magnetic anomaly (ADMAP2) compilations (Fretwell et al., 2013; Scheinert et al., 2016; Golynsky et al., 2017).

Besides these onshore observations and data, the post-breakup geological history is also recorded indirectly within the fills of sedimentary basins in the Riiser-Larsen Sea. These basins are isolated from their neighbours to the east and west by basement ridges. Astrid Ridge (Fig. 1) is a magmatic and volcanic ridge whose construction accompanied continental breakup and early seafloor spreading and continued at its northern end until at least 145 Ma, the age of oceanic lithosphere on which it rests (Leinweber and Jokat, 2012). Gunnerus Ridge (Fig. 1) formed in continental crust during relocation of a sheared segment of the Jurassic and early Cretaceous plate boundary from east to west Gondwana as the site of seafloor spreading between the two switched from the west Somali Basin to the Enderby Basin at around 133 Ma (Tuck-Martin et al., 2018).

2. AEROGEOPHYSICAL DATA

Extensive new aerogeophysical datasets were collected with the Alfred Wegener Institute's two Basler aircraft, Polar 5 and Polar 6, flying out of the Belgian station Princess Elisabeth in the 2013-14 and 2014-15 seasons (Fig. 1). The data were collected during the fourth stage of the GEA (Geodynamic evolution of East Antarctica) project, an ongoing collaboration between the Federal Institute for Geosciences and Natural Resources and the Alfred Wegener Institute, Helmholtz Centre for Polar and Marine Research. In total, close to forty thousand kilometres of gravity, radar, and magnetic data were collected for GEA-IV. Here, we present and discuss the gravity and radar data that are useful for evaluating the sources and transport pathways of sediments that are now preserved offshore in the Riiser-Larsen Sea. The magnetic data are presented and interpreted by Ruppel et al. (2018).

2.1. Radar

Large quantities of new radar data were collected using AWI's airborne EMR (Elektromagnetisches Reflexionssystem; Nixdorf et al., 1999). The system sends signal bursts with a frequency of 150 MHz and amplitude of 1.6 kW, toggling between durations of 60 ns and 600 ns with the aim of returning high-resolution images of both the internal structure and the bed of ice as much as 4 km thick. After 7-fold stacking and conversion from two-way travel time to depth, the dataset can be used to calculate distances between the aircraft and the top surface of the ice and its subglacial interface. These can be used together to determine ice thickness, and, with GPS determinations of flight level, ellipsoidal heights of the ice sheet surface and subglacial interface.

A GPS equipment failure led to the loss of radar capability on one flight in the 2013-14 season, and recurrent EMR signal problems led to the collection of unusable data on a further seven flights to the region north of the Yamato (Queen Fabiola) Mountains during the 2014-15 season. To make up for these losses, in part of the study region we use data gathered with AWI's EMR instrument during a EUFAR-funded flight in the 2010-11 season (Callens et al., 2014). Elsewhere, we sampled values from BEDMAP2 along our flight lines (Fretwell et al., 2013). After adjusting our bed depths to the GL04C geoid (Foerste et al., 2008) used for BEDMAP2, we then gridded the data set using minimum curvature rules for a regular 3 km grid spacing. The resulting basal topography is shown in Figure 2b. Example radargrams are shown in Figure 3.

2.2. Gravity

New free-air gravity data were collected as part of GEA-IV in 2013-14 with the Alfred Wegener Institute's LaCoste and Romberg/ZLS AirSea gravimeter (serial number S56) and in 2014-15 with the institute's Gravimetric Technology GT2A gravimeter (serial number 28). The International Gravity Standardization Net tie to Princess Elisabeth airfield (for the 2013-14 and 2014-15 data) was completed using AWI's LaCoste and Romberg portable gravimeters G744 and G877 via Novolazarevskaya Station (absolute measurement by Mäkinen, pers. comm. to Yildiz et al, 2017), visited before and after both campaigns. The 2013-14 data were collected at constant elevations, constrained by the capabilities of the AirSea gravimeter. Unpredictable broken and multi-level cloud in the 2013-14 season led to considerable data loss owing to multiple flight level changes on some profiles. Consequently, crossover errors within the AirSea data set are only determined along fragments of two tie lines and are not numerous enough to be statistically meaningful. At face value, these crossover values in the range 0-7 mGal suggest the instrument performed according to expectations. In contrast, along track data recovery with the GT2A gravimeter exceeded 95% owing to its capability to operate reliably during climb and descent. A 100 s filter length and flight speeds of 120-140 knots imply along-track half-wavelength resolution in the range 3.0-3.6 km. Where weather conditions permitted, data with this instrument were collected at a constant ice separation of 600 m. Crossover determinations within the GT2A data set are more numerous (90 to tie lines), the raw data returning a mean crossover error of -0.15 mGal and standard deviation of 2.50 mGal, suggesting this gravimeter too performed satisfactorily. These data are combined with older data acquired using S56 in 2006 and 2010 (Nogi et al. 2013; Mieth, 2014) to generate the grid in Figure 4b. After internal levelling, the S56 data were levelled to the GT2A data set. Simple Bouguer gravity anomalies (Fig. 4c) were calculated using ice, seawater, and crustal densities of 900, 1020 and 2670 kgm^{-3} without any terrain correction.

3. INTERPRETATION

3.1. Bed topography

Figure 2 shows that the overall pattern in subglacial topography is one of strong contrast between a plateau in the south, with highland peaks in and around Sør Rondane exceeding 3000 m above sea level, and coastal plains reaching a maximum depth around 960 m below sea level.

West of the Belgica Mountains, the coastal plain lies at an average of 380 m below sea level and gives way to the inland plateau at 1000-1500 m above sea level via a 2000-3000 m high escarpment (e.g. Fig. 2d, Profile 1). The mountains of Sør Rondane crop out on the seaward face and crest of the escarpment. A straight ESE-trending valley cuts the subglacial surface about 100 km south of the escarpment, coincident with part of the magnetically-defined Schirmacher-Rondane lineament of Ruppel et al. (2015). Hanging and overdeepened valleys can be interpreted from the grid in the areas between and immediately south of the mountains. These features record a phase of alpine glaciation and furthermore suggest that the escarpment relief hosting them was already in place at the time the ice sheet started to accumulate in the run-up to the Eocene-Oligocene transition.

The picture east of the Belgica Mountains is different (Fig. 2d, Profile 4). Here, the coastal plain dips somewhat irregularly inland, starting close to sea level a short distance behind the grounding line, and eventually dropping to around 150 m below sea level just north of a ~100 km length of east-striking escarpment. This escarpment, of around 1100-1500 m height, bends southwards at its western end to continue inland at lower elevations for at least another 150 km. The Yamato (Queen Fabiola) Mountains crop out from a north-striking spur to the north of the east-striking segment of escarpment. Together, this spur and the south-trending segment of the escarpment lie along strike from the Riiser-Larsen Peninsula (Fig. 1) and its offshore continuation, the submarine Gunnerus Ridge, suggesting they share a deeper geological control.

The ~150 km wide area between the Yamato (Queen Fabiola) Mountains and Sør Rondane presents a coastal plain with seaward and landward terraces at ~480 m and ~180 m below sea level (Fig. 2d, Profile 3). Further inland, the subglacial topography rises up landwards to 1700 m via a series of isolated rises, the most prominent of which bears outcrop at the Belgica massif.

The Belgica massif is separated from Sør Rondane to the west by a 15-20 km wide trough beneath the West Ragnhild glacier, which we refer to as the West Ragnhild trough. BEDMAP2 (Fretwell et al., 2013) shows the trough as a continuous feature north of Belgica Mountains. Our new radio echo sounding data show it also to continue until at least 100 km south of the mountains (Fig. 2c, Profile 2), where it passes out of the region of our survey. Along the way, the depth of the trough floor rises from its deepest point at least 1300 m below sea level (Callens et al., 2014) via a set of overdeepened sections, which the grid suggests to be individually 10-15 km long and between 150 and 350 m deep, to depths within a few hundred metres either side of sea level in a saddle near the Belgica Mountains. Averaging and smoothing of bed depths picked from the better-imaged trough flanks results in the narrow trough floor in the saddle being depicted at around 200 m above sea level in the grid (Fig. 2b). However, inwards of the flanks numerous EMR picks are made below sea level, and the steep sides of the unimaged parts of the trough leave little doubt that a narrow swath of its floor lies well below sea level (Fig. 3a). The current picture of the West Ragnhild trough is thus one of a canyon at least 350 km long, 15-20 km wide, and up to 1600 m deep, whose floor is likely to lie below sea level all along its length. The trough runs straight in a NNW orientation between 74°S and 71.2°S where, having passed the great escarpment on its western side, it bends sharply NW to continue to the grounding line. This section of the trough may be related to a pre-existing tectonic grain, as its NW trend is repeated in a separate ridge and trough lying 50 km to the south. The bend at 71.2°S coincides with the deepest of the overdeepened sections, and marks the northwards change from a deep rough bed to a smoother shallower bed first observed by Callens et al. (2014). Side valleys feeding into the West Ragnhild trough appear to be structurally controlled on the basis of their linearity and consistent northeasterly strike on both sides of the trough. Segments of the valleys at the western side of the trough are preserved as hanging valleys that permit ice drainage only along short (<100 km) tributaries to the West Ragnhild glacier (Rignot et al., 2011). The West Ragnhild trough and glacier at the present day thus drain only the eastern fringes of Sør Rondane and the plateau south of it.

Further west, inland of the great escarpment, very little about the bed was interpretable from BEDMAP2 (Fig. 2a) in which elevations over a large area were based on very sparse radio echo sounding data and a low-resolution inverse gravity model (Fretwell et al., 2013). Mieth and Jokat (2014) interpreted magnetic anomaly data to suggest that this region's upper crustal structural grain is oriented NW-SE. Figure 2 shows that relief with this trend is present, but by no means dominant, in the subglacial landscape. More prominently, the new data reveal the presence of a network of subglacial valleys reaching depths as much as 600 m below the surrounding topography. These valleys are sinuous, and thus appear less strongly controlled by geological structures than the West Ragnhild trough and its tributaries. The valleys are 15-30 km wide and usually V-shaped in cross section (Figs. 2b, 3b). The valleys converge at acute angles that close towards the southwest. The overall slopes of the great majority of these valley floors are towards the southwest. Consistent with the possibility of landscape preservation outlined above, these observations support the interpretation of a fluvial landscape with southwest-directed drainage. In the easternmost ~50 km of the data set, the floors of some of the valleys slope towards the east, suggesting the presence of a south-trending drainage divide to the catchment of the West Ragnhild trough (Fig. 2c). The apparent connectivity of these short east-sloping valley floor segments with the floors of the much longer southwest-sloping valleys suggest that this divide formed by local capture of southwest-flowing streams.

In more detail, the floors of the remaining parts of the valley system also do not slope monotonously downwards to the southwest, but instead feature local overdeepened (by ~100-150 m) segments (e.g. Fig. 3c). These observations are consistent with the valleys' modification by glacial erosion and deposition processes. As none of the valleys presently correlates with any present-day ice stream, and their orientation is perpendicular to the coastward ice flow direction (Rignot et al., 2011), we conclude that this modification occurred during an alpine glaciation phase that pre-dated establishment of the modern state of the ice sheet.

3.2. Free-air gravity

The free-air gravity anomalies, as expected, display strong coherency with basal topography interpreted from the EMR data. This coherency is well evident over the great escarpment of Sør Rondane and in the branching pattern of valleys south of the mountains (Fig. 4b). These valleys are not interpretable in the AntGG data set (Scheinert et al., 2016), which in this region is based on widely-spaced Soviet data (Leitchenkov et al, 2008). Free-air anomaly troughs are centred over the valley axes, their shapes mirroring those in the EMR bed topography, suggesting an origin by erosion into largely homogeneous rocks with no strong geological structural control.

The West Ragnhild trough anomaly is much sharper and deeper than in the AntGG dataset and, like the branching valleys south of Sør Rondane, its close mimicry of the EMR-based bed topography suggests its relief to be controlled dominantly by erosion. Its depth and shape through the saddle next to the Belgica Mountains are closely similar to those immediately north and south, supporting the interpretation that even in the saddle the trough floor lies below sea level. In the north, the free-air anomaly low associated with the trough continues for at least 30 km seawards of the grounding line. Beneath the ice shelf, it is likely therefore that the trough continues as a sediment-filled feature like that imaged immediately south of the grounding line by Callens et al. (2014). From the GT2A data set's southernmost crossings of the trough, the free-air anomaly low bends into a SE orientation, suggesting the trough may adopt a southeasterly strike just north of 73°40′ S. This impression is consistent with the orientation of a broad free-air low in the AntGG data set (Fig. 4a), whose greater extent also suggests that the SE-striking segment of the trough might continue towards 75°S, 35°E.

3.3. Bouguer Anomaly

The long wavelength signal in the Bouguer anomaly data set is one of increasing values northwards, towards the extended continental margin of Antarctica (Fig. 4c). This is consistent with increasing gravitational acceleration due to increasingly-shallow mantle rocks with densities exceeding 2670 kgm^{-3} beneath the crust, which we expect both to thin northwards as a result of tectonic extension, and to flex upwards in response to the reduced loading by the thinning ice sheet. At shorter wavelengths, this increase shows a sharp (~30 km) step at the crest of the great escarpment. This wavelength is not typical of flexural topography (Watts and Moore, 2017), but might still be seen as consistent with a step-like contrast in Moho depth across a crustal-scale basin-bounding fault coincident with the escarpment. Seismic estimates of crustal thickness in the region are too sparse to reveal details of its Moho topography, but outcrop geology (e.g. Jacobs et al., 2015) and magnetic anomalies (Ruppel et al. 2018) do not permit the interpretation of any such fault near the surface. A more plausible interpretation is that the upper crust north of the escarpment crest has been thinned more by erosion than that further south. There is no comparable sharp contrast in Bouguer gravity values across the Yamato (Queen Fabiola) Mountains.

The West Ragnhild trough appears as a subdued linear low in the Bouguer anomaly data. North of the bend in the anomaly at 71.2°S, this low is confidently interpretable in terms of a trough fill of subglacial sediments of lower density than the rocks the trough is cut into. Further south, localised more strongly negative Bouguer values correlate to segments of the trough floor without radar reflections. We regard these negative anomalies as artefacts related to the erroneously shallow interpolated bed values in the EMR data grid.

In contrast, some of the larger valleys south of Sør Rondane are marked by ~20 mGal relative Bouguer highs. If these highs were consequences of systematically poorly-picked bed depths in the EMR data, then the valley floor picking error would be too large to have gone unnoticed, in the region of 200 m. A more plausible alternative interpretation is that the valleys are cut into an uppermost crustal layer with a density less than the crustal reduction density of 2670 kgm^{-3} used for the Bouguer correction. A density of less than 2670 kgm^{-3} could be characteristic of low-grade metasedimentary rocks like the greenschist-facies supracrustal rocks widely reported from Sør Rondane (Jacobs et al. 2015). Figure 5 illustrates such a scenario using a two-dimensional model of gravity anomalies sampled from the grid. The accompanying model of magnetic anomalies sampled from the data set of Ruppel et al. (2018) uses small susceptibilities in its uppermost layer that are also typical of metasedimentary rocks.

4. EROSION AND SEDIMENTATION ACROSS THE CONTINENTAL MARGIN

4.1 Background

Before this study, retreat of the great escarpment of Dronning Maud Land has only been addressed in relation to interpretations of denudation from low temperature geochronology data. As at many other margins worldwide, the distribution of mineral cooling data from Dronning Maud Land means such interpretations are not unequivocal (Braun and van der Beek, 2004). Näslund's (2001) interpretation of post-breakup denudation in western Dronning Maud Land (Jacobs et al., 1992; 1995) in terms of erosional retreat of an originally-tectonic fault scarp thus remains be tested using complementary approaches.

At the escarpment's further eastern reaches, Krohne (2017) generated apatite fission track data from a small area of Sør Rondane to interpret its denudation history. Together with regional geological constraints, they interpreted cooling at 215-180 Ma in terms of the removal of 2.8 km fill from a Permo-Triassic intracontinental basin in response to tectonic uplift at the margins of extensional basins formed during Gondwana breakup. Following this, those authors interpret ongoing extensional tectonism leading to reburial of Sør Rondane in a local basin until 140 Ma, perhaps responding to landward migration of a flexurally-controlled drainage divide, followed by renewed denudation at 140-120 Ma, quiescence until 40 Ma, and localised denudation accompanying strong rock cooling until present. Added to these ideas, in the previous sections we used our new datasets to interpret how at the time of ice sheet glaciation, more than 100 million years following the onset of seafloor spreading in the Riiser-Larsen Sea, a significant escarpment and drainage divide existed at the continental margin of eastern Dronning Maud Land. We build on these starting observations and ideas in the next section, which examines further products of erosion at the continental margin: the sediments deposited offshore of it.

4.2 Sedimentation and basins of the Riiser-Larsen Sea

Leitchenkov et al. (2008) interpreted the stratigraphy revealed in a network of seismic reflection profiles from the Riiser-Larsen Sea (Fig. 6a). The framework of their interpretation is a set of regional reflection surfaces. Below the seafloor, the uppermost of these surfaces is dated to the onset of regional glaciation at 34 Ma, because it marks the change from sub-parallel and parallel to more varied reflectivity patterns (Kuvaas et al., 2004). Ages are assigned to five deeper surfaces on the basis of their onlaps onto oceanic crustal basement. The age of the deepest, the top of acoustic basement, varies from place to place owing to its creation by extension of pre-existing continental crust (>160-164 Ma) or by seafloor spreading processes (<160-164 Ma). The age of the deepest sedimentary surface is assigned based on its interpretation by Leitchenkov et al (2008) as a breakup unconformity marking the onset of seafloor spreading at 160-164 Ma, as determined from magnetic anomaly data from the conjugate Mozambique Basin (Leinweber and Jokat, 2012). The remaining three ages are more confidently applicable because the basement age is directly constrained by magnetic isochron interpretations at 144 Ma, 122 Ma, and 51 Ma.

Total sediment thickness variation in the Riiser-Larsen Sea reveals the presence of two main basins on the continental rise. The western basin, labelled A in Figure 6a, lies between Astrid

Ridge and the mouth of the West Ragnhild trough near 20°E. It is subdivided into western and eastern parts by an unnamed basement high near 16°E. Sediment fill is thickest in its eastern part. The lack of any major offshore sediment fan or long onshore feeder trough allows us to assume that sediments accumulated in basin A from two local sources. The first was the adjacent continental margin, which has been limited southwards by the great escarpment since Gondwana breakup. The second, in late Jurassic times only, was active volcanoes along the magmatic Astrid Ridge. In the eastern basin, B, the total sediment thickness increases from west to east, reaching maxima in excess of 6.5 km in two lobes that narrow towards the mouth of the West Ragnhild trough at 24°E on the continental slope. The lobes are suggestive of the trough having hosted sediment transport processes to basin B.

Castelino et al. (2016) presented estimates of sedimentation rate histories at two points in basin B and at one in the shallow part of basin A. All three reveal fast accumulation in late Jurassic and early Cretaceous times and in the run-up to post-Eocene perennial glaciation of East Antarctica. For a more wide-ranging picture of the sedimentation history, Figure 6b shows normalised accumulation histories that have been determined from 59 locations spaced at 25 km intervals along four of Leitchenkov et al.'s (2008) interpreted profiles. The majority of the profiles show a three-stage pattern, with an initial rapid phase of accumulation in late Jurassic through early Cretaceous times followed first by a long period of very slow accumulation, and later by accelerated sediment accumulation accompanying the onset of regional glaciation in Cenozoic times. Figure 6b shows that this pattern is broadly consistent with the conclusions of Krohne's (2017) cooling-based denudation study. In detail, however, whilst Leitchenkov et al.'s (2008) seismic stratigraphy should be finely enough resolved to test Krohne's (2017) interpretation of basin filling onshore at ~160-140 Ma, there is no obvious signal of such an event having stalled offshore accumulation. We propose an alternative interpretation of this reheating that draws on a lull in the rate of filling in the volcaniclastic basin east of Astrid Ridge at ~160-140 Ma (Fig. 6b), at a time when the rest of basins A and B were filling rapidly. If this lull is interpreted to represent uplift and emergence of Astrid Ridge and the neighbouring part of basin A in response to activity of the Astrid Ridge mantle plume, then the accompanying increase of regional heat flow might be postulated as the cause of reheating at Sør Rondane.

4.3 Sediment volume balance test of great escarpment erosion history

As noted above, rapid late Jurassic sediment accumulation (Fig. 6b) indicates extensional tectonics during Gondwana breakup led to the development and erosion of significant tectonic topography at the continental margin of the Riiser-Larsen Sea. Further to this, we expect the Riiser-Larsen Sea to be well suited for testing more detailed ideas about the great escarpment's role in this erosion because sediment transport to it has only ever been possible across the Princess Ragnhild Coast; along-slope transport is restricted by the Astrid and Gunnerus ridges. Figure 6c presents a gross check of this expectation by comparing estimates of clast volumes deposited in and sourced to the Riiser-Larsen Sea since 164 Ma.

To generate these estimates, we again used Leitchenkov et al's (2008) sediment thickness data set. The thicknesses are based on average interval velocities from sonobuoy records that enable a coarse depth migration of travel times in the network. Based on an error analysis of similar data sets further east around the East Antarctic margin, uncertainty in these thicknesses may reach 25% of the calculated values (Whittaker et al, 2013), with possible extra unquantifiable uncertainty attached to the fact that the onlap-defined stratigraphy can only be indirectly verified by extrapolation of the DSDP/ODP-tied stratigraphy in the Weddell Sea (Rogenhagen et al., 2004; Lindeque et al., 2013; Huang and Jokat, 2016). Using the 25% thickness uncertainty, and assuming average porosity to 7 km depth lies in the range 12-21% (based on Bahr et al.'s, 2001 compaction coefficients for sand and mud) the volume of clasts in basin A sediments amounts to something in the range between 2.9×10^5 and 4.2×10^5 km^3. Subtracting the proportion of volcaniclastic material in the sub-basin neighbouring Astrid Ridge, whose volume we estimate on the basis of its proportion of chaotic or transparent reflectivity to amount to about 0.65×10^5 km^3, we estimate that basin A contains a volume of $2.25\text{-}3.55 \times 10^5$ km^3 in clasts that can be assumed to have been eroded from the adjacent continental margin seaward of the great escarpment. We compare this volume to that of a now-eroded rock body that had been 600 km long and 150 km wide, the same as the present-day area between the shelf and Sør Rondane, whose bottom surface lay at around 0.4 km below sea level (Fig. 2b) and whose top surface lay 2-3 km (cf. the denudation estimates of Jacobs et al. (1995) and Krohne (2017)) above the present-day height (1.3-3.1 km) of the mountains, making it something in the range 3.7-6.5 km thick. Assuming negligible porosity prior to erosion, the volume of this eroded rock lay in the range $3.3\text{-}5.9 \times 10^5$ km^3. In view of the expected loss of some of the eroded material by passage through basin A, to deposition on the continental shelf, or to dissolution, this volume is consistent with the estimated total volume of clasts in basin A sediments (Fig. 6c).

The volume balance exercise thus enables us to conclude that continental margin topography developed during and soon after Gondwana breakup was eroded to form sediments that were subsequently deposited in the western Riiser-Larsen Sea. In the following section, we adopt this conclusion as an assumption that allows more detailed analysis of the erosion and sedimentation history.

5. DISCUSSION

5.1 Great escarpment erosion: mechanism and history

The slight increase in sedimentation rates after the Eocene (Fig. 6b) and modest alteration of the fluvial landscape south of Sør Rondane suggest that the ice sheet facing basin A did not experience a long-lived or widespread warm-based phase of activity during its build up. Based on this, we assume that the escarpment is currently stationary and has been ever since 34 Ma. Immediately beforehand, the period 122-34 Ma saw very slow sediment accumulation in Basin A. Escarpment retreat in that period is thus likely to have been at modest rates, and not to have led to capture of any large drainage catchment. Similarly, the same observations for that period allow us to rule out that the region was affected by significant changes in dynamic topography, tectonic relief generation, or large climatic changes. The 165-122 Ma period, in contrast, saw the accumulation of around two-thirds of the fill of Basin A, suggesting an early period of more meaningful escarpment retreat. These conclusions are also consistent with the observation that the regional subglacial landscape is characterized by a single escarpment and plain (Fig. 2), except perhaps in the narrow margin segment occupied by the Belgica mountains and West Ragnhild trough.

The present day great escarpment lies 150 km inland of the continental shelf break. To achieve this separation during a single phase of escarpment retreat starting with breakup at 165 Ma and ending with cold-based glaciation at 34 Ma would require a long-term backwearing rate of 1.1 km/Myr. This resembles both the long-term escarpment retreat rate estimated for the Namibian escarpment by Cockburn et al. (2000), and maximum plausible long-term backwearing rates in the landscape evolution model experiments presented by Braun (2018). However, the long-term retreat rate required to fill basin A by two-thirds in the 165-122 Ma period would be about 2.3 km/Myr. With reference to the results of Braun's (2018) one-dimensional landscape evolution modelling, achieving this by backwearing alone would require a physically unreasonable combination of conditions; an unusually long characteristic length, unusually high transport by hillslope processes, and unusually large lithospheric effective elastic thickness. Following Brown et al. (2002), Cockburn et al. (2000) and Fleming et al. (1999), an alternative to this implausibility is to accept the occurrence of a significant (that is, approximately equal in sediment yield) component of downwearing over an area between the escarpment and an inland drainage divide that existed prior its formation. The existence of such a divide raises the possibility that the fluvial valleys in the subglacial landscape south of Sør Rondane may have been draining towards the southwest since as long ago as early-to-middle Jurassic times.

5.2 Sediments transported by the 'Ragnhild river'

At something in the range 6.8-9.7 x 10^5 km^3, the volume of clastic material in basin B is between one and a half and three times greater than that eroded from the margin in the west and now resting in basin A. Figure 6b shows that this material accumulated most rapidly during Callovian-Aptian times. Unlike in basin A, it is not possible to relate this signal to the erosion of breakup-related margin relief because of its size. Although the Belgica and Yamato (Queen Fabiola) mountains present fragments of escarpments that might testify to such a process, the short length of the margin segment they occupy mean that the expected volume material eroded from in front of them would be less, not more, than that west of the West Ragnhild trough.

Instead, the accumulation of basin B sediments in lobes that fan out from the mouth of the West Ragnhild trough suggests they were transported to the margin by a river whose valley was later glacially altered to form the trough. The trough originates well inland of the Belgica and Yamato escarpment fragments, beyond which BEDMAP2 data, although sparse, suggest this 'Ragnhild river' catchment may have occupied much of western Enderby Land northwest of the older (Permo-Triassic; Thomson et al., 2013) tectonic relief of the East Antarctic rift system. Whilst the catchment's relatively large area potentially explains the volume of sediment encountered in basin B, there is a lack of evidence for Jurassic tectonic relief-forming processes that would explain the sediments' accumulation in the short period following Riiser-Larsen Sea breakup. This accumulation signal can instead be related to regional climate change, in which an arid pre-breakup continental interior became humid in response to the development of the new ocean between the Weddell and Riiser-Larsen seas. There is no available rock record from the Ragnhild river catchment to test such an idea. Paleocirculation modelling (Sellwood and Valdes, 2003) however raises the possibility of humidification in accompaniment to seaway development across Gondwana, albeit for an outdated plate kinematic model in which this seaway is considerably wider by Late Jurassic times than more modern studies show.

6. CONCLUSIONS

- New aerogeophysical data reveal details of the topography of the East Antarctic Ice Sheet and its bed in the region south of Sør Rondane for the first time.
- Sør Rondane lies on a 2-3 km high escarpment. The subglacial topography of the plateau inland of this escarpment is interpretable as that of a pre-existing fluvial landscape. The fluvial drainage pattern shows that the escarpment existed as a drainage divide prior to ice sheet glaciation.
- The eastern margin of Sør Rondane is the West Ragnhild trough, an imposing subglacial canyon just 15-20 km wide but over 350 km long and exceeding 1.6 km deep in places. Almost the entire length of the trough floor in the new data lies below sea level.
- The relief of the great escarpment around Sør Rondane, the West Ragnhild trough, and the fluvial landscape southwest of them were locally enhanced by alpine glaciation at some time prior to the ice sheet glaciation of the region, which probably dates from 34 Ma.
- A volume balance exercise to assess erosion and deposition of sediments that were transported from continental East Antarctica to the western Riiser-Larsen Sea across the Princess Ragnhild Coast supports concepts of great escarpment formation during rapid early erosion of topography formed by tectonic processes at the time of continental breakup.
- Compared to the results of published landscape evolution models, the Jurassic-early Cretaceous rate of escarpment retreat implied for this erosion to occur by backwearing alone is unfeasibly fast. Backwearing was likely accompanied by downwearing to such an extent that both may have yielded similar quantities of eroded material.
- The requirement for a pre-existing inland drainage divide to focus the coastal downwearing component suggests some features of the regional relief may be even older than late Jurassic.
- The concentration of sediments in the eastern Riiser-Larsen Sea in lobes fanning out from the West Ragnhild trough reveals the trough's pre-glacial history as the valley of a major river draining parts of the East Antarctic interior.

- Rapid accumulation of the sediment lobes in the immediate aftermath of continental breakup suggests the development of an ocean led to the late Jurassic onset of a wetter climate in the continental interior of East Gondwana.
- The first order relief of eastern Dronning Maud Land dates at least from the aftermath of Gondwana breakup in late Jurassic times. The region has been characterised by high topography ever since.

ACKNOWLEDGEMENTS

We gratefully acknowledge Kenny Matsuoka and EUFAR (http://www.eufar.net) for their roles in enabling the collection of EMR data in 2010/11. The GEA programme is jointly funded by the Alfred Wegener Institute, Helmholtz Centre for Polar and Marine Research (AWI), and the Federal Institute for Geosciences and Natural Resources (BGR). GEA-IV would not have been possible without the scientific, technical and logistical expertise of Tobias Binder, Veit Helm, the technicians of AWI and FIELAX, Wayne Hewison of Canadian Microgravity, the crews of Kenn Borek Air Ltd, Alain Hubert of the Polar Foundation, and the support crews at Novo Runway and Princess Elisabeth station. For further scientific and technical support at AWI, we are grateful to Rashpal Singh and Jude Castelino. Two anonymous reviewers provided generously detailed and constructive feedback for which we are extremely grateful.

REFERENCES

1. Bahr, D. B., Hutton, E. W., Syvitski, J. P., & Pratson, L. F., 2001, Exponential approximations to compacted sediment porosity profiles. *Computers & Geosciences*, *27*(6), 691-700.
2. Beaumont, C., Kooi, H., and Willett, S., 2000, Coupled tectonic-surface process models with applications to rifted margins and collisional orogens, in Summerfield, M.A., ed., Geomorphology and global tectonics: Chichester, John Wiley, p. 29–55.
3. Braun, J., 2018, A review of numerical modeling studies of passive margin escarpments leading to a new analytical expression for the rate of escarpment migration velocity, Gondwana Research, 53, 209-224.
4. Braun, J., van der Beek, P., 2004. Evolution of passive margin escarpments: what can we learn from low-temperature thermochronology. Journal of Geophysical Research 109, F04009. http://dx.doi.org/10.1029/2004JF000147.
5. Brown, R. W., Rust, D. J., Summerfield, M. A., Gleadow, A. J., & De Wit, M. C., 1990, An Early Cretaceous phase of accelerated erosion on the south-western margin of Africa: Evidence from apatite fission track analysis and the offshore sedimentary record. *International Journal of Radiation Applications and Instrumentation. Part D. Nuclear Tracks and Radiation Measurements*, *17*(3), 339-350.
6. Brown, R., Summerfield, M., Gleadow, A., 2002, Denudational history along a transect across the Drakensberg Escarpment of southern Africa derived from apatite fission track thermochronology. Journal of Geophysical Research 107, 2350. http://dx.doi.org/10.1029/2001JB000745.
7. Callens, D., Matsuoka, K., Steinhage, D., Smith, B., Witrant, E. and Pattyn, F., 2014, Transition of flow regime along a marine-terminating outlet glacier in East Antarctica. Cryosphere, 8, 867–875, (doi:10.5194/tc-8-867-2014)

8. Callens, D., Thonnard, N., Lenaerts, J., Van Wessem, J. M., Van De Berg, W. J., Matsuoka, K., & Pattyn, F., 2015, Mass balance of the Sør Rondane glacial system, East Antarctica. *Annals of Glaciology*, *56*, 63-69.
9. Campanile, D., Nambiar, C.G., Bishop, P., Widdowson, M., Brown, R., 2008, Sedimentation record in the Konkan–Kerala basin: implications for the evolution of the Western Ghats and the Western Indian passive margin. *Basin Research*, 20, 3–22.
10. Castelino, J. A., Eagles, G., and Jokat, W., 2016, Anomalous bathymetry and palaeobathymetric models of the Mozambique Basin and Riiser Larsen Sea, *Earth and Planetary Science Letters*, *455*, 25-37.
11. Cockburn, H.A.P., Brown, R.W., Summerfield, M.A., and Siedl, M.A., 2000, Quantifying passive margin denudation and landscape development using a combined fission track thermochronology and cosmogenic isotope analysis approach, Earth and Planetary Science Letters, 179, 429-435.
12. DeConto, R.M., and Pollard, D., 2003, Rapid Cenozoic glaciation of Antarctica induced by declining atmospheric CO2. *Nature* 421, 245-249.
13. Eagles, G, and König. M., 2008, A model of plate kinematics in Gondwana breakup, *Geophysical Journal International*, 173, 703-717.
14. Fleming, A., Summerfield, M.A., Stone, J.O., Fifield, L.K., and Cresswell, R.G., 1999, Denudation rates for the southern Drakensberg escarpment, SE Africa, derived from in-situ produced cosmogenic ^{36}Cl: initial results, Journal of the Geological Society of London, 156, 209-212.
15. Fretwell, P., et al., 2013, Bedmap2: improved ice bed, surface and thickness datasets for Antarctica, *The Cryosphere* 7.1.
16. Foerste, C., Schmidt, R., Stubenvoll, R., Flechtner, F., Meyer, U., König, R., Neumayer, H., Biancale, R., Lemoine, J.-M., Bruinsma, S., Loyer, S., Barthelmes, F., and Esselborn, S., 2008, The GeoForschungsZentrum Potsdam/Groupe de Recherche de Geodesie Spatiale satellite-only and combined gravity field models: EIGEN-GL04S1 and EIGEN-GL04C. Journal of Geodesy, 82, 6, 331-346, doi:10.1007/s00190-007-0183-8.
17. Gilchrist, A. R., and Summerfield, M.A., 1990, Differential denudation and flexural isostasy in formation of rifted-margin upwarps, Nature, 346, 739–742.
18. Gilchrist, A.R., and Summerfield, M.A., 1994, Tectonic models of passive margin evolution and their implications for theories of long-term landscape evolution, in Kirkby, M.J., ed., Process models and theoretical geomorphology: Chichester, John Wiley and Sons, p. 55–84.
19. Golynsky, A.V., et al., 2017, ADMAP-2: Magnetic anomaly map of the Antarctic, DOI:10.22663/ADMAP.V2
20. Guillocheau, F. D. Rouby, C. Robin, C. Helm, N. Rolland, C. Le Carlier de Veslud, and J. Braun, 2012, Quantification and causes of the terrigeneous sediment budget at the scale of a continental margin: A new method applied to the Namibia–South Africa margin, Basin Res., 24, 3–30, doi:10.1111/j.1365-2117.2011.00511.x.
21. Gunnell, Y., Fleitout, L., 1998. Shoulder uplift of the Western Ghats passive margin, India: a denudational model. *Earth Surface Processes and Landforms*, 23, 391–404.
22. Heimsath, A.M., Chappell, J., Finkel, R.C., Fifield, K., Alimanovic, A., 2006, Escarpment erosion and landscape evolution in southeastern Australia. Special Paper 398: Tectonics, Climate, and Landscape Evolution. *Geological Society of America*., pp. 173–190.
23. Holbourn, A, et al., 2005, Impacts of orbital forcing and atmospheric carbon dioxide on Miocene ice-sheet expansion, *Nature*, 438, 483-487.
24. Huang, X, and W Jokat., 2016, Sedimentation and potential venting on the rifted continental margin of Dronning Maud Land, *Marine Geophysical Research*, 37, 313-324.
25. Jacobs, J., Hejl, E., Wagner, G. A., & Weber, K., 1992, Apatite fission track evidence for contrasting thermal and uplift histories of metamorphic basement blocks in western Dronning Maud Land. *Recent Progress in Antarctic Earth Science, Terrapub, Tokyo*, 323-330.
26. Jacobs, J., Ahrendt, H., Kreutzer, H., & Weber, K., 1995, K-Ar, ^{40}Ar-^{39}Ar and apatite fission-track evidence for Neoproterozoic and Mesozoic basement rejuvenation events in the Heimefrontfjella and Mannefallknausane (East Antarctica), *Precambrian Research*, *75*, 251-262.
27. Jacobs, J., Elburg, M., Läufer, A., Kleinhanns, I. C., Henjes-Kunst, F., Estrada, S., Ruppel, A.S., Damakse, D., Montero, P., and Bea, F., 2015, Two distinct late Mesoproterozoic/early Neoproterozoic basement provinces in central/eastern Dronning Maud Land, East Antarctica: The missing link, 15–21 E, *Precambrian Research*, *265*, 249-272.

28. Jamieson, S.S.R., and Sugden, D.E., 2008. Landscape evolution of Antarctica. In: Cooper, A.K., Barrett, P.J., Stagg, H., Storey, B., Stump, E., Wise, W., 10th ISAES editorial team (Eds.), Antarctica: a keystone in a changing world: Proceedings of the 10th International Symposium on Antarctic Earth Sciences. The National Academies Press, Washington D.C, pp. 39–54.
29. King, L. C., *1953, Cannons of landscape evolution,* Geol. Soc. Am. Bull., 64, 721–752.
30. Koppes, M. N., & Montgomery, D. R., 2009, The relative efficacy of fluvial and glacial erosion over modern to orogenic timescales, *Nature Geoscience*, *2*, 644-647.
31. Kounov, A., Niedermann, S., de Wit, M., Viola, G., Andreoli, M., Erzinger, J., 2007, Present denudation rates at selected sections of the South African escarpment and the elevated continental interior based on cosmogenic ^{3}He and ^{21}Ne. *South African Journal of Geology*, 110, 235–248.
32. Krohne, N., 2017, *From active to passive margins: the basin and highland evolution of the Weddell Sea sector, East Antarctica*, (Doctoral dissertation, University Bremen).
33. Kuvaas, B., Kristoffersen, Y., Leitchenkov, G., Guseva, J., & Gandjukhin, V., 2004, Seismic expression of glaciomarine deposits in the eastern Riiser Larsen Sea, Antarctica. *Marine Geology*, *207*, 1-15.
34. Leinweber, V. T., & Jokat, W., 2012, The Jurassic history of the Africa–Antarctica corridor—new constraints from magnetic data on the conjugate continental margins. *Tectonophysics*, *530*, 87-101.
35. Leitchenkov, G., Guseva, J., Gandyukhin, V., Grikurov, G., Kristoffersen, Y., Sand, M., Golynsky, A., and Aleshkova, N., 2008, Crustal structure and tectonic provinces of the Riiser-Larsen Sea area (East Antarctica): results of geophysical studies. *Marine Geophysical Researches*, *29*, 135-158.
36. Lindeque, A., Martos, Y. M., Gohl, K., & Maldonado, A., 2013, Deep-sea pre-glacial to glacial sedimentation in the Weddell Sea and southern Scotia Sea from a cross-basin seismic transect. *Marine Geology*, *336*, 61-83.
37. Mandal, S.K., Lupker, M., Burg, J.-P., Valla, P.G., Haghipour, N., Christl, M., 2015, Spatial variability of ^{10}Be-derived erosion rates across the southern Peninsular Indian escarpment: a key to landscape evolution across passive margins. *Earth and Planetary Science Letters* 425, 154–167.
38. Matmon, A., Bierman, P., and Enzel, Y., 2002, Pattern and tempo of great escarpment erosion, *Geology*, 30, 1135-1138.
39. Mieth, M., 2014, *Aerogeophysical constraints for the geodynamic evolution of Dronning Maud Land, East Antarctica* (Doctoral dissertation, University Bremen).
40. Mieth, M., & Jokat, W., 2014, New aeromagnetic view of the geological fabric of southern Dronning Maud Land and Coats Land, East Antarctica, *Gondwana Research*, *25*, 358-367.
41. Näslund, J. O., 2001, Landscape development in western and central Dronning Maud Land, East Antarctica. *Antarctic Science*, *13*, 302-311.
42. Nixdorf, U., Steinhage, D., Meyer, U., Hempel, L., Jenett, M., Wachs, P., & Miller, H., 1999, The newly developed airborne radio-echo sounding system of the AWI as a glaciological tool. *Annals of glaciology*, *29*, 231-238.
43. Nogi, Y., Jokat, W., Kitada, K., & Steinhage, D., 2013, Geological structures inferred from airborne geophysical surveys around Lützow-Holm Bay, East Antarctica. *Precambrian Research*, *234*, 279-287.
44. Ollier, C.D., 1984, Morphotectonics of continental margins with great escarpments, in Morisawa, M., and Hack, J.T., eds., *Tectonic geomorphology*: Boston, Unwin Hyman, p. 3–25.
45. Partridge, T. C. and Maud, R.R., 1987, Geomorphic evolution of southern Africa since the Mesozoic, *South African Journal of Geology,* 90, 179–208.
46. Pattyn, F. 2010, Antarctic subglacial conditions inferred from a hybrid ice sheet/ice stream model, *Earth and Planetary Science Letters*, 295, 451-461.
47. Riedel, S., Jacobs, J., & Jokat, W., 2013, Interpretation of new regional aeromagnetic data over Dronning Maud Land (East Antarctica). *Tectonophysics*, *585*, 161-171.
48. Rignot, E., Mouginot, J., & Scheuchl, B., 2011, Ice flow of the Antarctic ice sheet. *Science*, *333*, 1427-1430.
49. Rogenhagen, J., Jokat, W., Hinz, K., and Kristoffersen, Y., 2004, Improved Seismic Stratigraphy of the Mesozoic Weddell Sea, *Marine geophysical researches*, 25, 265282, doi:10.1007/s11001-005-1335-y
50. Rouby, D., Bonnet, S., Guillocheau, F., Braun, J., Biancotto, F., Robin, C., Dauteuil, O., Gallagher, K., 2009, Sediment supply to the Orange sedimentary system over the last 150 Ma: an evaluation from erosion/sedimentation balance, *Marine and Petroleum Geology*, 26, 782–794.

51. Ruppel, A. S., Läufer, A., Jacobs, J., Elburg, M., Krohne, N., Damaske, D., & Lisker, F., 2015, The Main Shear Zone in Sør Rondane, East Antarctica: Implications for the late-Pan-African tectonic evolution of Dronning Maud Land. *Tectonics*, *34*, 1290-1305.
52. Ruppel, A.S., Jacobs, J., Eagles, G., Läufer, A., and Jokat, W., 2018, New geophysical data from a key region in East Antarctica: estimates for the spatial extent of the Tonian Oceanic Arc Super Terrane (TOAST), *Gondwana Research*, 59, 97-107. https://doi.org/10.1016/j.gr.2018.02.019
53. Rust, D. J., & Summerfield, M. A., 1990, Isopach and borehole data as indicators of rifted margin evolution in southwestern Africa. *Marine and Petroleum Geology*, *7*, 277-287.
54. Sacek, V., Braun, J., & Beek, P., 2012, The influence of rifting on escarpment migration on high elevation passive continental margins. *Journal of Geophysical Research: Solid Earth*, *117*, B04407.
55. Scheinert, M., et al., 2016, New Antarctic gravity anomaly grid for enhanced geodetic and geophysical studies in Antarctica. *Geophysical Research Letters*, *43*, 600-610.
56. Sellwood, B.W., and Valdes, P.J., 2006, Mesozoic climates: General circulation models and the rock record, *Sedimentary Geology*, 190, 269-287.
57. Shevenell, A. E., Kennett, J. P., & Lea, D. W., 2004, Middle Miocene southern ocean cooling and Antarctic cryosphere expansion. *Science*, *305*(5691), 1766-1770.
58. Siegert, M. J., Carter, S., Tabacco, I., Popov, S., & Blankenship, D. D., 2005, A revised inventory of Antarctic subglacial lakes, *Antarctic Science*, *17*(3), 453-460.
59. Thomson, S.N., Reiners, P.W., Hemming, S.R., and Gehrels, G.E., 2013, The contribution of glacial erosion to shaping the hidden landscape of East Antarctica, *Nature Geoscience*, 6, 203-207, doi:10.1038/NGEO1722
60. Tuck-Martin, A., Adam, J., and Eagles, G., 2018, New plate kinematic model and tectono-stratigraphic history of the East African and West Madagascan margins, Basin Research, in press, doi:10.1111/bre.12294
61. Watts, A.B., & Moore, J.D.P., 2017, Flexural isostasy: Constraints from gravity and topography power spectra. Journal of Geophysical Research: Solid Earth, 122, 8417–8430. https://doi.org/10.1002/2017JB014571
62. Wilson, D.S., Jamieson, S.S.R., Barrett, P.J., Leitchenkov, G., Gohl, K., and Larter, R.D., 2012, Antarctic topography at the Eocene-Oligocene boundary, *Palaeogeography, Palaeoclimatology, Palaeoecology*, 335-336, 24-34
63. Whittaker, J. M., Goncharov, A., Williams, S. E., Müller, R. D., & Leitchenkov, G., 2013, Global sediment thickness data set updated for the Australian-Antarctic Southern Ocean. *Geochemistry, Geophysics, Geosystems*, *14*, 3297-3305.
64. Wildman, M., Brown, R., Beucher, R., Persano, C., Stuart, F., Gallagher, K., Schwanethal, J. and Carter, *A.,* 2016, The chronology and tectonic style of landscape evolution along the elevated Atlantic continental margin of South Africa resolved by joint apatite fission track and (U-Th-Sm)/He thermochronology, *Tectonics*, 35, 511–545, *doi:*10.1002/2015TC004042.
65. Yildiz, H., Forsberg, R., Tscherning, C. C., Steinhage, D., Eagles, G., & Bouman, J., 2017, Upward continuation of Dome-C airborne gravity and comparison with GOCE gradients at orbit altitude in east Antarctica. *Studia Geophysica et Geodaetica*, *61*, 53-68.

FIGURES

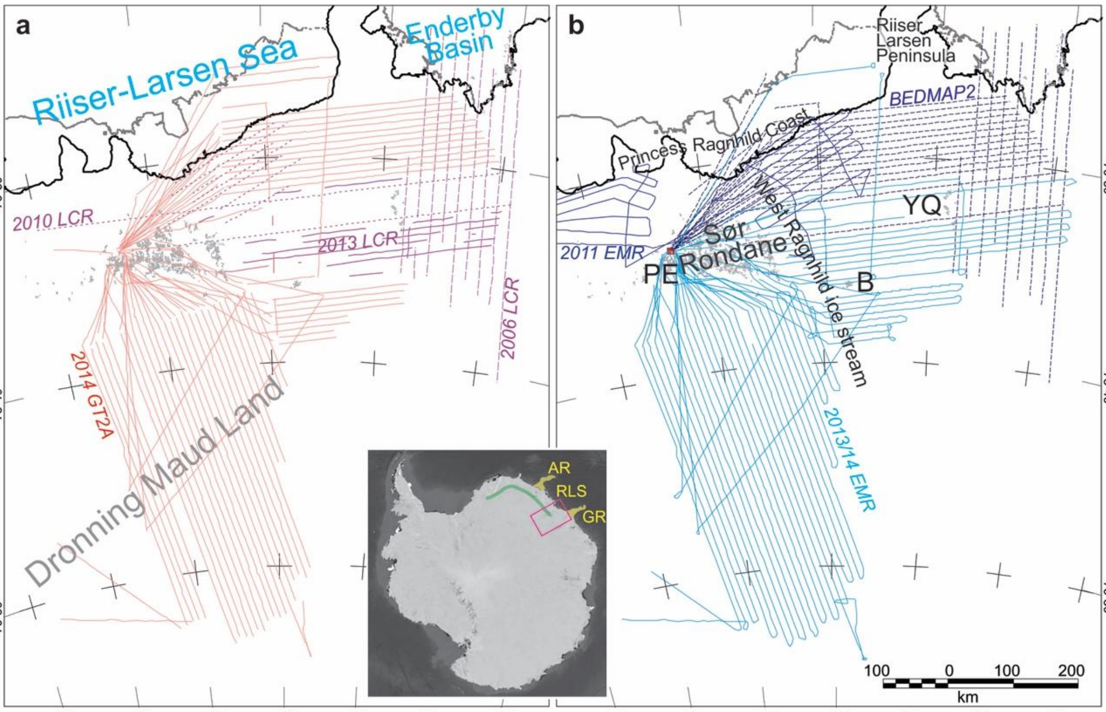

FIGURE 1: Study location and flight lines used. a) Data used for compilation of free-air gravity anomaly grid; GT2A: Gravimetric Technologies gravimeter; LCR: Lacoste & Romberg/ZLS AirSea gravimeter. b) Data used for compilation of sub-ice topography grid. B: Belgica Mountains; PE: Princess Elisabeth station; YQ: Yamato (Queen Fabiola) Mountains. Inset: Antarctica, the survey area (red box) and the great escarpment of Dronning Maud Land (green line). Yellow: basement ridges at the margins of the Riiser-Larsen Sea (RLS). AR: Astrid Ridge, GR: Gunnerus Ridge.

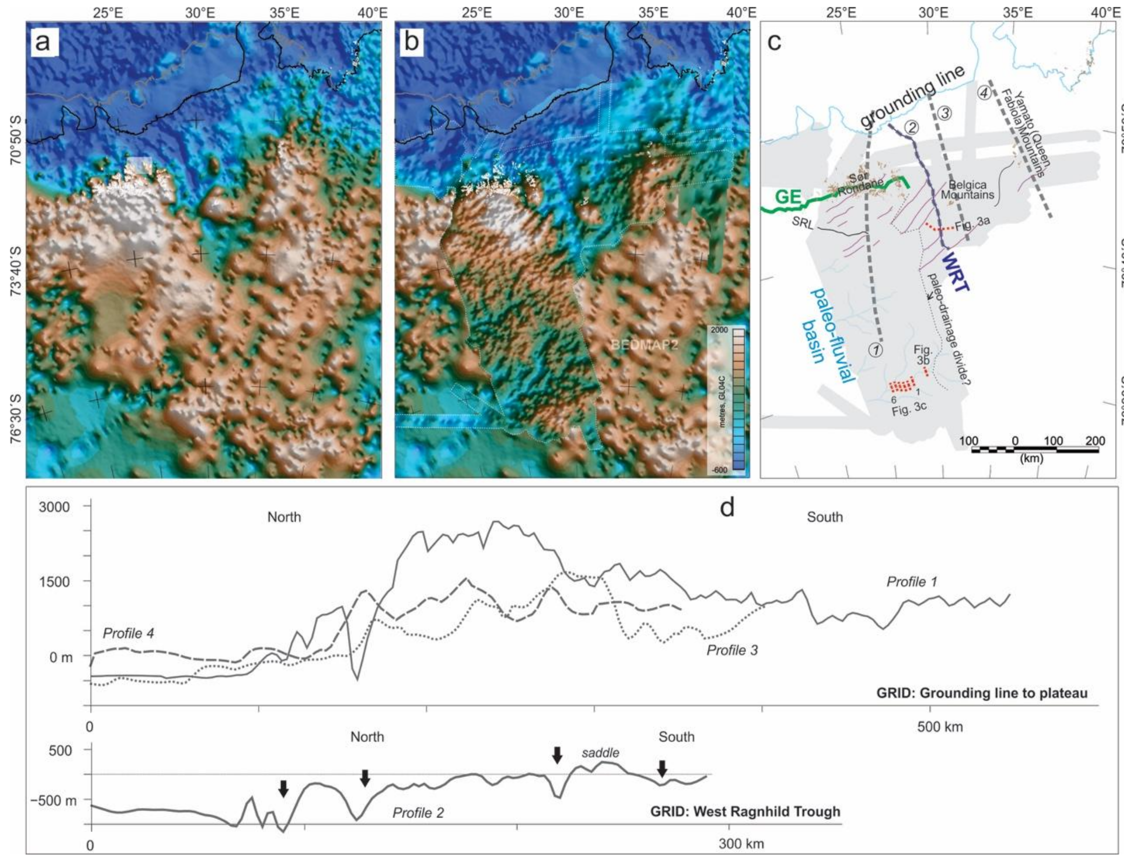

Figure 2: a) BEDMAP2 bed depth estimates; b) bed depth estimates from new EMR data set (inside the dotted outline) with BEDMAP2 in the background, c) interpretation (see text for details). Grey fill: area covered by new data at 10 km line spacing. Green line / GE: great escarpment (the gridded 2.2 km contour along the escarpment face); dark blue line / WRT: West Ragnhild trough; black line / SRL: valley associated with part of Schirmacher-Rondane Lineament; light blue lines: valley networks with fluvial branching characteristics; mauve lines: straight, NE-trending lineaments. Grey dashed lines: lines of grid profiles shown in (d). Red dotted lines: locations of radargrams of Figure 3. d) Profiles over the grid of bed elevation. Black arrows: overdeepened sections along valley profiles.

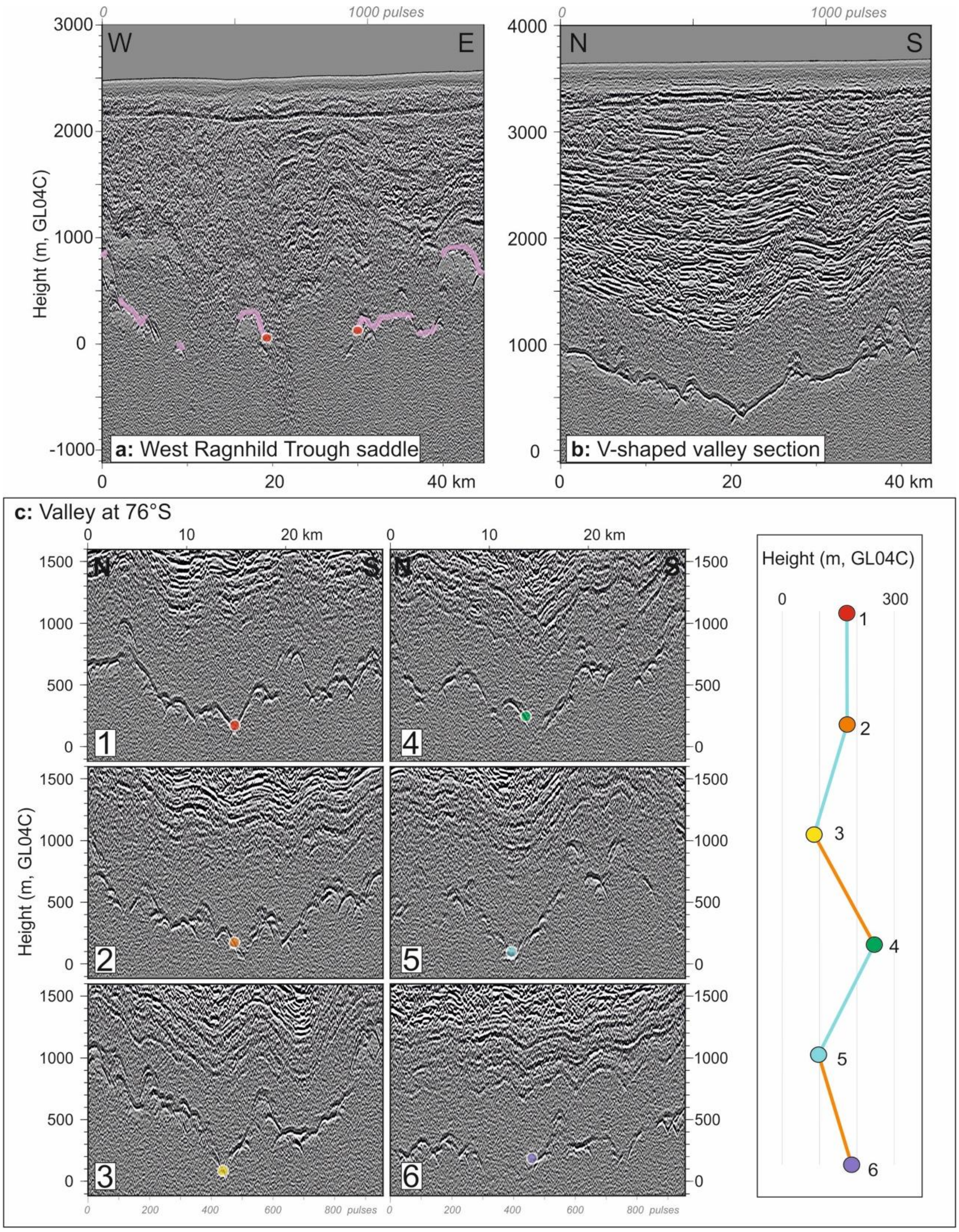

Figure 3: a) Radargram over the saddle in the West Ragnhild trough (at ~25 km distance) between Sør Rondane and Belgica Mountains. Pink lines are interpreted bed reflections, red discs show the deepest picks at the trough flanks between which the trough floor is not imaged but likely to lie below sea level; b) radargram over mid-stream section of a v-shaped valley south of Sør Rondane, c) Six radargrams showing valley floor picks (coloured discs) further downstream in the same valley as (b), and a height profile from those picks. Uphill-westwards segments are coloured orange.

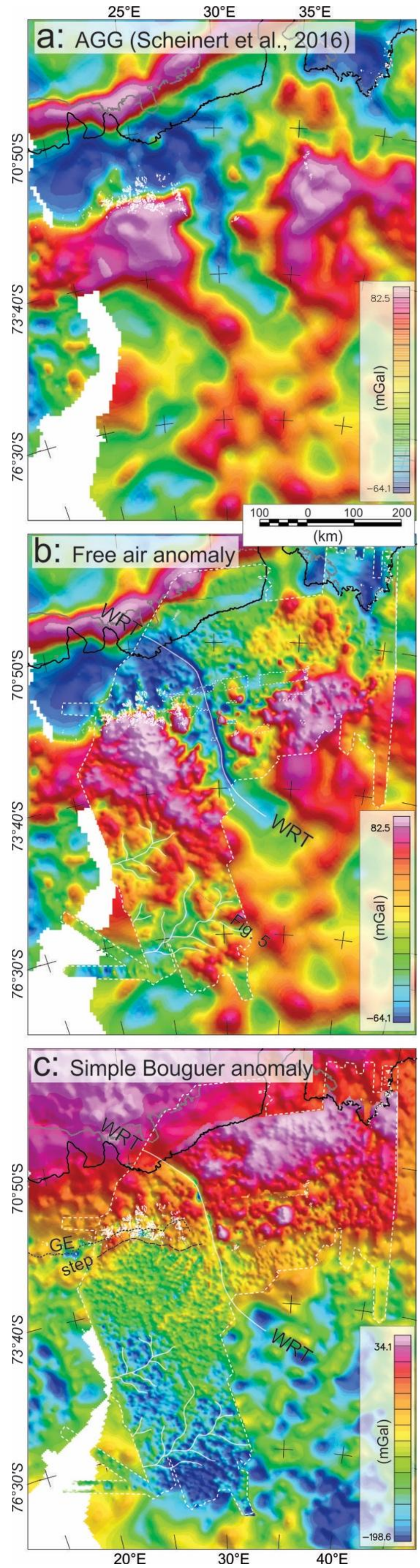
a: AGG (Scheinert et al., 2016)
25°E
30°E
35°E
70°50'S
73°40'S
76°30'S
82.5
(mGal)
−64.1
100
0
100
200
(km)
b: Free air anomaly
WRT
WRT
Fig. 5
70°50'S
73°40'S
76°30'S
82.5
(mGal)
−64.1
c: Simple Bouguer anomaly
WRT
WRT
GE
step
70°50'S
73°40'S
76°30'S
34.1
(mGal)
−198.6
20°E
30°E
40°E

Figure 4: a) Free air anomalies in the AntGG free-air anomaly dataset of Scheinert et al. (2016). b) Newly compiled free-air anomaly data within the dotted outline, AntGG outside it. White lines: valleys interpreted from EMR data. WRT: West Ragnhild trough. c) new simple Bouguer anomalies overlain on complete Bouguer anomaly dataset of Scheinert et al. (2016). GE: gridded 2.2 km contour on escarpment face, from Figure 2; 'step': short wavelength marginwards increase of Bouguer anomaly at the escarpment crest.

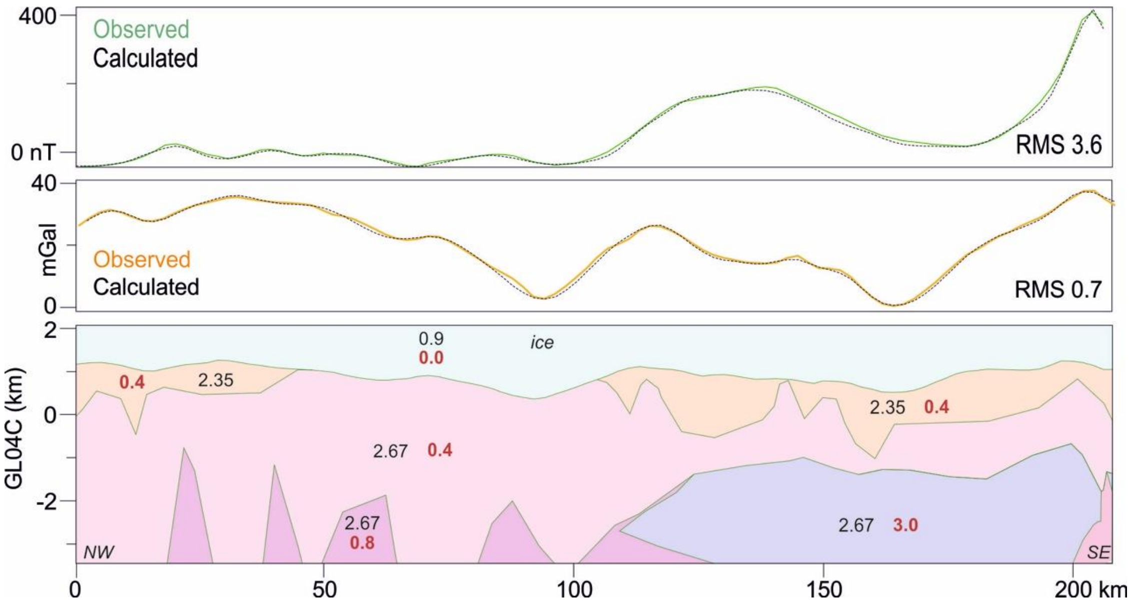

FIGURE 5: Two-dimensional gravity (centre) and magnetic (top) anomaly models for a profile running NW-SE, perpendicular to one of the main valleys (at 95 km) south of the Sør Rondane escarpment (see Fig. 4b for location). Red numbers indicate SI magnetization values x10^{-3}. Black numbers indicate densities in thousands of kgm^{-3}. Given the very sparse regional outcrop constraints, model body variability is interpreted in the text only in terms of metamorphic grade.

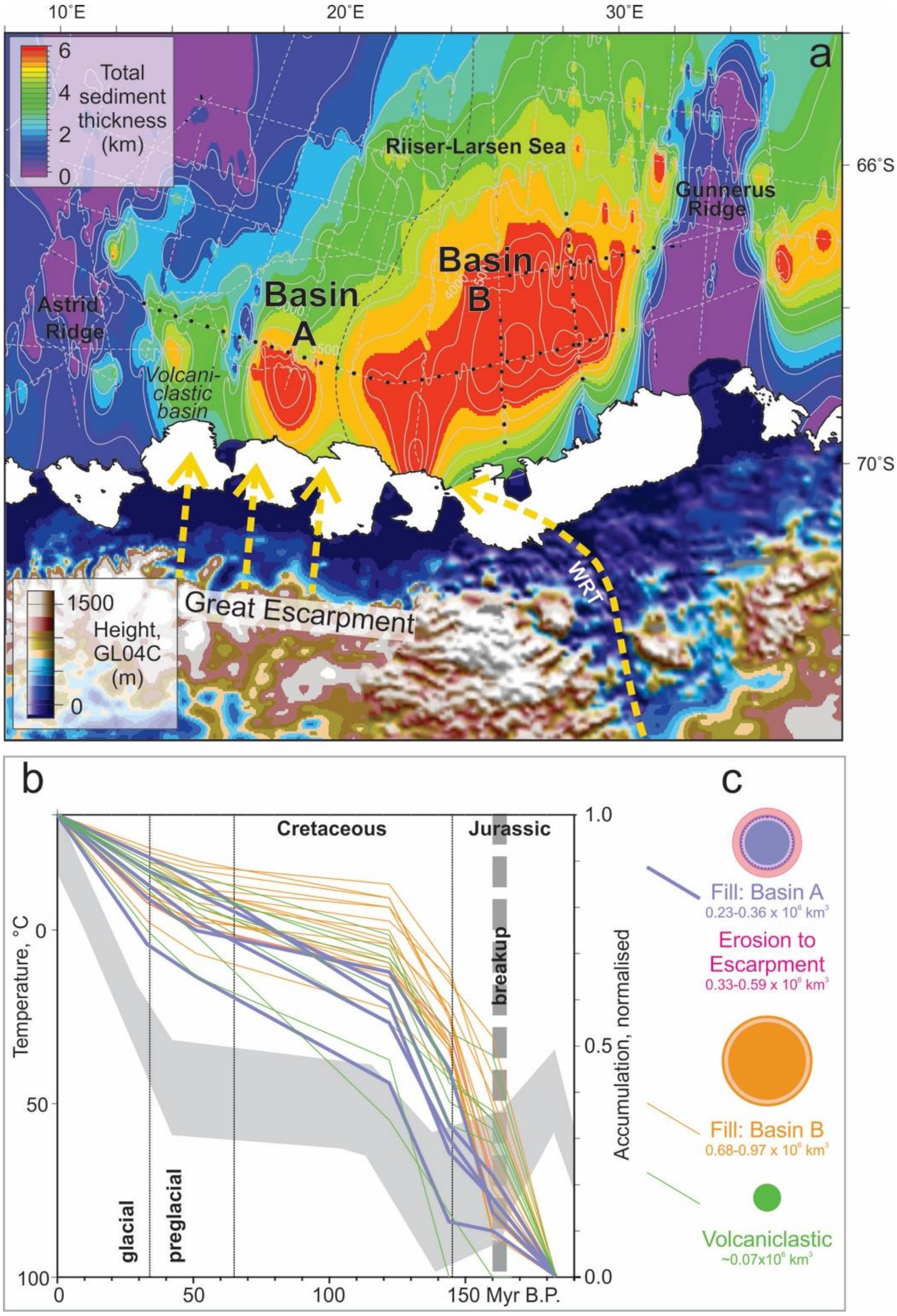

FIGURE 6: a) Total sediment thickness distribution in the Riiser-Larsen Sea (Leitchenkov et al. 2008) and bed topography of neighbouring Sør Rondane region. Dashed lines show locations of seismic data constraints. WRT: West Ragnhild trough. b) Sediment accumulation histories at sites spread throughout the Riiser-Larsen Sea (black discs in (a)) and low-temperature thermal history (background grey envelope) of Sør Rondane after Krohne (2017). c) maximum and minimum estimated volumes of clastic component of Riiser-Larsen Sea sediments and of material eroded from seawards of the great escarpment.